



OPEN

Cobalt isatin-Schiff-base derivative of MOF as a heterogeneous multifunctional bio-photocatalyst for sunlight-induced tandem air oxidation condensation process

Majid Rouzifar¹, Sara Sobhani^{1✉}, Alireza Farrokhi¹ & José Miguel Sansano²

A sunlight-induced tandem air oxidation-condensation of alcohols with *ortho*-substituted anilines or malononitrile for the efficient synthesis of benz-imidazoles/-oxazoles/-thiazoles, or benzylidene malononitrile catalyzed by Co-isatin-Schiff-base-MIL-101(Fe) as a heterogeneous multifunctional bio-photocatalyst is reported. In these reactions, Co-isatin-Schiff-base-MIL-101(Fe) acts both as a photocatalyst, and a Lewis acid to catalyze the reaction of the in-situ formed aldehydes with *o*-substituted anilines or malononitrile. A significant decrease in the band gap energy and an increase in the characteristic emission of MIL-101(Fe) after functionalization with cobalt Schiff-base according to the DRS analysis and fluorescence spectrophotometry, respectively, indicate that the photocatalytic effectiveness of the catalyst is associated primarily to the synergetic influence of Fe–O cluster and Co-Schiff-base. EPR results obviously pointed out that Co-isatin-Schiff-base-MIL-101(Fe) is capable of creating $^1\text{O}_2$ and O_2^- as active oxygen species under visible light irradiation. Using an inexpensive catalyst, sunlight irradiation, air as a cost-effective and abundant oxidant, and a low amount of the catalyst with recoverability and durability in ethanol as a green solvent, make this methodology as an environmentally friendly process with energy-saving organic synthetic strategies. Furthermore, Co-isatin-Schiff-base-MIL-101(Fe) displays excellent photocatalytic antibacterial activity under sunlight irradiation against *E. coli*, *S. aureus* and *S. pyogenes*. Based on our knowledge, this is the first report of using a bio-photocatalyst for the synthesis of the target molecules.

Currently, from the sustainable chemistry standpoint, decreasing environmental contamination and rising energy deficiency, are progressively concerned¹. Tandem reactions which contain two or more consecutive independent reactions implemented in a one-pot manner with no isolation and purification of the intermediates, diminish the number of reaction steps, the solvent and reagents usage and consequently decrease the waste production and energy consumption.

Development of simple methods for the synthesis of required organic intermediates or final products from readily available reagents constitutes a key challenge in the synthetic organic chemistry^{2,3}. Alcohols are considered as the most environmentally benign compounds, because of the readily availability, low cost, chance of being produced from renewable biomass resources, less poisoning, and ease of treatment, storage and transportation⁴. Therefore, the synthesis of organic compounds directly from alcohols by tandem organic process (TOP) has been known as an environmentally friendly chemical synthetic method⁵.

Although traditional thermal routes still have a significant role in current chemistry, a number of subsequent problems like waste byproducts formation due to some undesirable thermal side reactions urge to move towards using a renewable energy source^{6,7}. In this regard, mimicking the nature in the consumption of sunlight to yield nutrient and oxygen in the plants, leads chemists to employ this available, free-charge and renewable energy source for the activation of catalytic transformations⁸. The examples of using solar energy as the activator in the photocatalytic transformations involve the removal of drugs⁹, organic dyes and heavy metal ions from wastewater by photo-degradation or -reduction¹⁰, inhibition of air contaminants, hydrogen generation by water splitting as

¹Department of Chemistry, College of Sciences, University of Birjand, Birjand, Iran. ²Departamento de Química Orgánica, Facultad de Ciencias, Centro de Innovación en Química Avanzada (ORFEO-CINQA), Universidad de Alicante, Apdo. 99, 03080 Alicante, Spain. ✉email: ssobhani@birjand.ac.ir

well as chemical synthesis¹¹. Primary studies in this field involved the use of photocatalysts with wide band gap like titanium or zinc oxide^{12,13}. However, the big band gap and the fast recombination of electron–hole pairs cause low photocatalytic productivity and poor practicality. Moreover, the structure of traditional semiconductors, which are not matched, restricted their extra progress in the field of photocatalysis. Therefore, the discovering of efficient photocatalysts to substitute the conventional ones is highly demanded¹⁴.

Metal–organic frameworks (MOFs), a hybrid material with a three-dimensional crystalline structure, are discovering as a distinctive type of heterogeneous photocatalysts, due to their admirable photoexcitation and charge transition mechanism^{15–18}. The inherent light absorption of MOFs can be tuned by changing either the metal ions as network nodes or the conjugation amount in the organic ligands^{12,19–21}. In recent years, the use of MOFs for light-initiated oxidation reactions such as oxidation of saturated carbon–hydrogen bonds, hydroxylation of benzene, and selective oxidation of sulfides has been extensively documented^{22–24}. Furthermore, due to the individual structure of MOFs which contains diverse catalytic sites such as metal nodes, ligands and catalytic species encapsulated in the holes, they have been used as multifunctional catalysts in tandem reactions such as epoxidation–ring opening, Sonogashira Hagiwara–click and olefination–hydrogenation reactions^{25–27}. However, the use of MOF-based materials as multifunctional catalysts under light irradiation for the TOP reactions starting from alcohols are in the infancy stages^{28–34}.

In continue of our studies on the introducing new heterogeneous catalysts for the organic transformations^{35–37}, herein, in this paper, we have applied a MOF modified with cobalt-complex³⁸ [Co-isatin-Schiff-base-MIL-101(Fe)] as a new heterogeneous multifunctional bio-photocatalyst for the synthesis of benz-imidazoles/-oxazoles/-thiazoles, and benzylidene malononitrile by TOP starting from readily available alcohols. The photocatalytic antibacterial activity of Co-isatin-Schiff-base-MIL-101(Fe) against *E. coli*, *S. aureus* and *S. pyogenes* was also studied under sunlight illumination.

Experimental

General information. Chemicals were purchased from Merck Company. The reactions were monitored by TLC using silica-gel polygram SILG/UV254 plates. X-ray photoelectron spectroscopy (XPS) was done by a VG-Microtech Multilab 3000 spectrometer, equipped with an Al anode. The deconvolution of spectra was done by Gaussian Lorentzian curves. X-ray powder diffraction (XRD) was carried out on an Xpert Pro Panalytical diffractometer incorporating Cu K α radiation ($\lambda = 0.154 \text{ \AA}$). TEM images were obtained by a TEM microscope (Philips CM30). Field emission scanning electron microscopy (FESEM) images were obtained using a FESEM (model Mira 3-XMU). UV–Vis diffuse reflectance spectroscopy (UV–Vis-DRS, Shimadzu Co., Japan), FT-IR spectra were recorded on a Nicolet-Impact 400D spectrometer in the range of 400–4000 cm^{-1} . The cobalt catalyst percentage was measured using an OPTIMA 7300DV ICP analyzer. EPR data were achieved on a Bruker EMX (freq. 9.80 GHz, time 80 ms, modulation freq. 100 kHz). Experiments were performed under sunlight irradiation between 8.00 a.m. and 4.00 p.m. (July to August 2021, at $\sim 30 \text{ }^\circ\text{C}$).

Synthesis of Fe-MIL-101-isatin-Schiff-base. MIL-101(Fe)-NH₂ (0.13 g)³³ was added to a solution of isatin (0.147 g, 1 mmol) in ethanol (20 mL) and then refluxed for 1 day. The brown solid was centrifuged, washed with EtOH (3 \times 10 mL) and dried at 60 $^\circ\text{C}$ in a vacuum oven to give the brown isatin-Schiff-base-MIL-101(Fe).

Synthesis of Co-isatin-Schiff-base-MIL-101(Fe). Co(OAc)₂·4H₂O (0.05 g, 0.2 mmol) was added to a mixture of isatin-Schiff-base-MIL-101(Fe) (0.1 g) in ethanol (15 mL) and stirred under reflux conditions for 24 h. Then, the solid was centrifuged, washed with EtOH (3 \times 10 mL) and dried in a vacuum oven. The total amount of cobalt per gram of Fe-MIL-101-isatin-Schiff-base-Co was found to be 2.24 mmol by ICP analysis.

Typical method for photocatalytic oxidation of benzyl alcohol in the presence of Co-isatin-Schiff-base-MIL-101(Fe). A mixture of catalyst (1 mol%), benzyl alcohol (1 mmol), and EtOH (6 mL) was stirred in a glass tube under sunlight irradiation and air bubbling at $\sim 30 \text{ }^\circ\text{C}$. The reaction progress followed by TLC. After an appropriate time (Table 3), the catalyst was isolated by centrifugation and washed with ethanol. The solvent of the combined organic phase was evaporated under reduced pressure. The pure product was obtained by column chromatography.

General route for the synthesis of benz-imidazoles/oxazoles/thiazoles via Tandem photo-oxidation-condensation reaction from benzyl alcohols and o-phenylenediamines catalyzed by Co-isatin-Schiff-base-MIL-101(Fe). A mixture of Co-isatin-Schiff-base-MIL-101(Fe) (1.2 mol %, 5.3 mg), benzyl alcohol (1 mmol) and o-phenylenediamine/o-aminophenol/o-aminothiophenol (1 mmol) in ethanol (6 mL) was stirred at $\sim 30 \text{ }^\circ\text{C}$, while exposed to the sunlight, and air was bubbled into the reaction mixture (1 mL min⁻¹). The reaction progress followed by TLC. After an appropriate time (Table 5), the catalyst was isolated by centrifugation, washed with ethanol (3 \times 5 mL), and then reused in subsequent runs. The yellow product was obtained after addition of ice water to the remaining solution. The precipitated product was filtered and recrystallized in ethanol to provide the pure product.

Tandem photo-oxidation/Knoevenagel condensation reaction catalyzed by Co-isatin-Schiff-base-MIL-101(Fe). Benzyl alcohol (1 mmol) and malononitrile (1 mmol) were added to a glass tube containing Co-isatin-Schiff-base-MIL-101(Fe) (1.5 mol%) and EtOH (6 mL) equipped with a stirring bar. The reaction mixture was stirred at $\sim 30 \text{ }^\circ\text{C}$ with mild air flow under sunlight irradiation. After appropriate times (Table 8), as monitored by TLC (elution: n-hexane/ethyl acetate: 10:1), the catalyst was separated

by centrifugation. The solvent of the remaining solution was evaporated under vacuum to produce the crude product. The pure product was obtained by ethanol–water recrystallization.

Results and discussion

Synthesis and characterization of Co-isatin-Schiff-base-MIL-101(Fe). Co-isatin-Schiff-base-MIL-101(Fe)³⁸ was synthesized via post modification method (PSM) of MIL-101(Fe)-NH₂ (Fig. 1).

Figure 2 shows the PXRD pattern of the as-synthesized MIL-101(Fe)-NH₂ and the Co-isatin-Schiff-base-MIL-101(Fe). The well-defined diffraction peaks at 2θ of 9.2, 10.5, and 16.6° have revealed the high crystallinity of Fe-MIL-101-NH₂. The XRD pattern of Fe-MIL-101-isatin-Schiff-base-Co is shown diffraction peaks at 2θ of 9.2, 10.6, and 16.6°. The slight changes observed in the XRD of the functionalized sample compared to the original MOF are probably due to the creation of some defects in the catalyst structure during the functionalization reaction.

To further investigation of the presence and types of the elements expected for the Co-isatin-Schiff-base-MIL-101(Fe), X-Ray photoelectron spectroscopy (XPS) was performed as depicted in Fig. S1. C 1s spectrum represents four peaks corresponded to C=C (284.4 eV), C=N (285.4 eV), C-N (287.5 eV) and C=O (289.2 eV) (Fig. S1a)³⁹. The N 1s spectrum (Fig. S1b) consists of peaks at 398.5 and 400.6 eV, which are related to C=N and N-H bonds, respectively⁴⁰. Two peaks at 711.3 eV and 724.9 eV (Fig. S1c) for Fe 2p_{3/2} and Fe 2p_{1/2}, respectively, confirm the existence of Fe⁺³ in the MOF⁴¹. Presence of two pairs of distinct peaks in the high resolution XPS of Co 2p (Fig. S1d) at 781.3 (Co 2p_{3/2}) and 797.3 eV (Co 2p_{1/2}), indicates the existence of Co²⁺ in Co-isatin-Schiff-base-MIL-101(Fe)^{42,43}.

Morphology of Co-isatin-Schiff-base-MIL-101(Fe) and MIL-101(Fe)-NH₂ were established by field emission scanning electron microscopy and transmission electron microscopy (FESEM and TEM). As shown in Fig. 3, the morphology of MIL-101(Fe)-NH₂ remains nearly intact after PSM.

Based on EDX spectrum, elements including carbon, oxygen, nitrogen, iron and cobalt present in Co-isatin-Schiff-base-MIL-101(Fe) (Fig. 4). Investigation of EDX-mapping indicates a uniform distribution of these elements in the catalyst (Fig. 5).

Study of the FT-IR spectra of the as-synthesized MIL-101(Fe)-NH₂ and Co-isatin-Schiff-base-MIL-101(Fe) (Fig. 6a,c) ensured the successful construction of the targeting MOF. In the spectrum of MIL-101(Fe)-NH₂, the peaks at 1382–1430 (C=C) and 1501–1600 (C=O) cm⁻¹ are attributed to the 2-aminoterephthalate linkers (Fig. 6a). After PSM of MIL-101(Fe)-NH₂, some new peaks at around 1700 (C=O), 1628 (C=N) and 1332 (C-N) cm⁻¹ are formed, which could be attributed to the isatin-Schiff-base (Fig. 6b). Complex formation of isatin-Schiff-base in the isatin-Schiff-base-MIL-101(Fe) with cobalt is associated with the shift of vibration frequencies of C=O and C=N groups to the lower amounts (Fig. 6c).

Comparison of the N₂ adsorption–desorption of Co-isatin-Schiff-base-MIL-101(Fe) with MIL-101(Fe)-NH₂ (Fig. S2a,b) showed that the surface areas and total pore volumes are considerably reduced in Co-isatin-Schiff-base-MIL-101(Fe) (Table 1). The pore size distribution of the two samples is nearly identical (Fig. S2c,d). These results indicated the successful incorporation of Co (II) complexes into MIL-101(Fe)-NH₂ with uniform distribution.

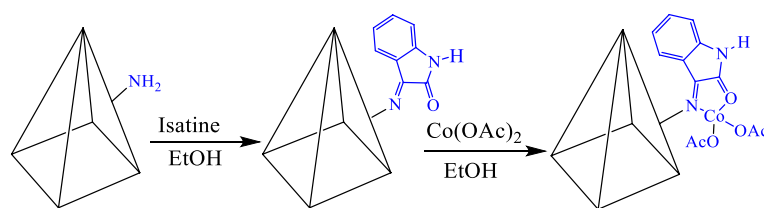


Figure 1. Synthetic route for the preparation of Co-isatin-Schiff-base-MIL-101(Fe).

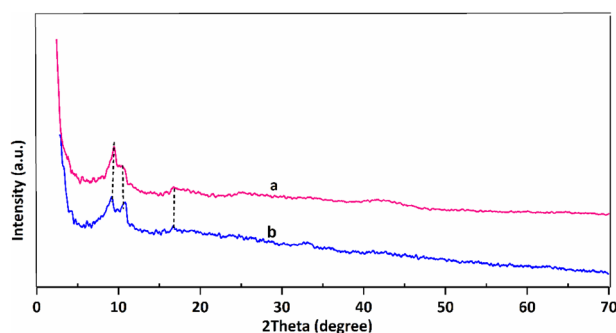


Figure 2. PXRD patterns of (a) MIL-101(Fe)-NH₂ and (b) Co-isatin-Schiff-base-MIL-101(Fe).

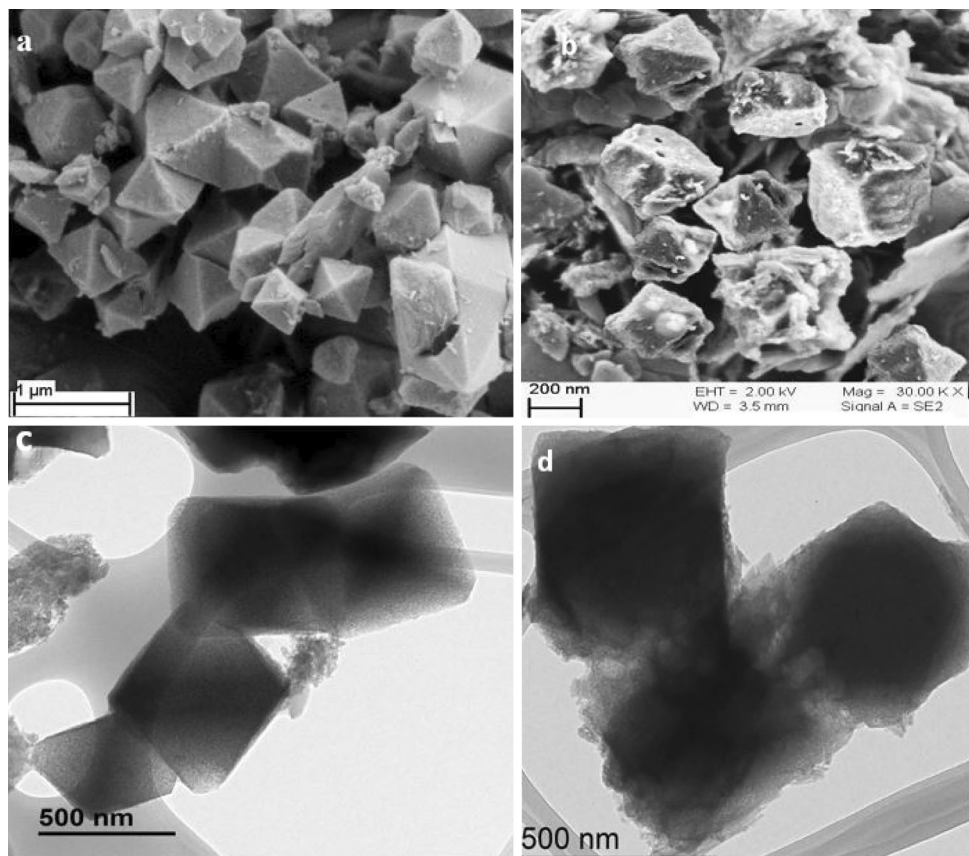


Figure 3. FESEM images of (a) MIL-101(Fe)-NH₂ and (b) Co-isatin-Schiff-base-MIL-101(Fe); TEM images of (c) MIL-101(Fe)-NH₂ and (d) Co-isatin-Schiff-base-MIL-101(Fe).

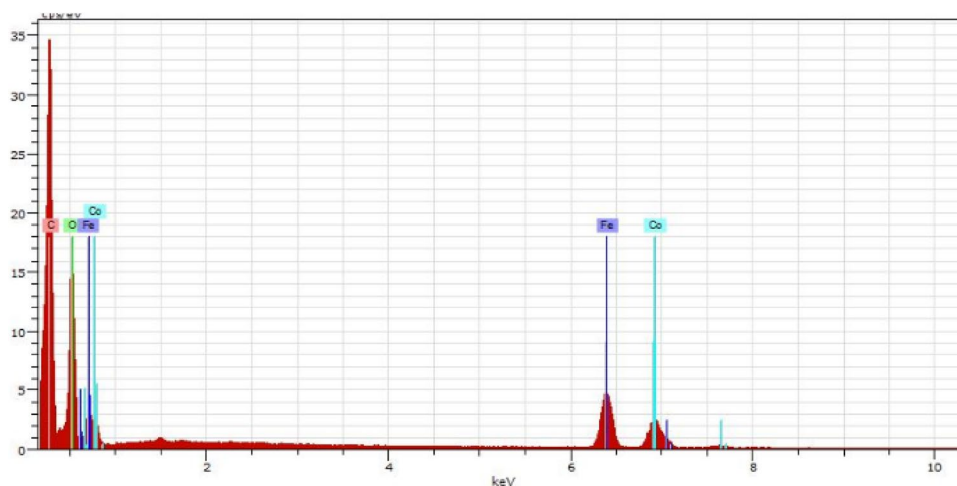


Figure 4. EDX spectrum of Co-isatin-Schiff-base-MIL-101(Fe).

The UV-Vis DRS spectrum of Co-isatin-Schiff-base-MIL-101(Fe) shows a broad absorption band in the visible light region (250–800 nm) compared with MIL-101(Fe)-NH₂ and isatin-Schiff-base-MIL-101(Fe) (Fig. 7). These results showed that Co-isatin-Schiff-base-MIL-101(Fe) can be excited in the visible region, due to the existence of Fe–O clusters in conjunction with cobalt Schiff-base, which facilitates the π – π transitions. The DRS analysis showed a significant decrease in the band gap energy (E_g) of MIL-101(Fe)-NH₂ from 2.23⁴⁴ to 2.03 eV after modification by isatin and 1.7 eV after complex formation with cobalt (Fig. 8).

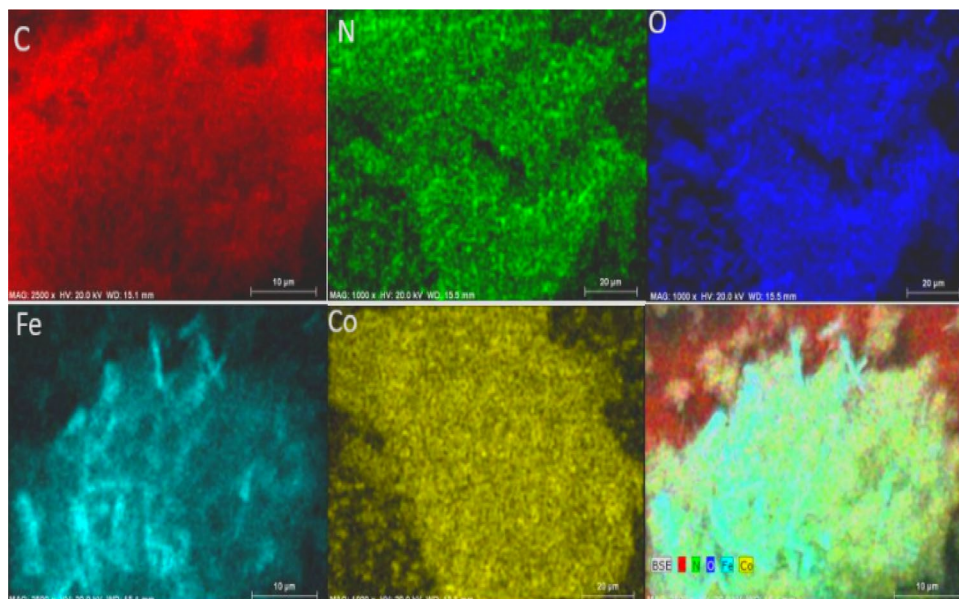


Figure 5. EDX mapping images of Co-isatin-Schiff-base-MIL-101(Fe).

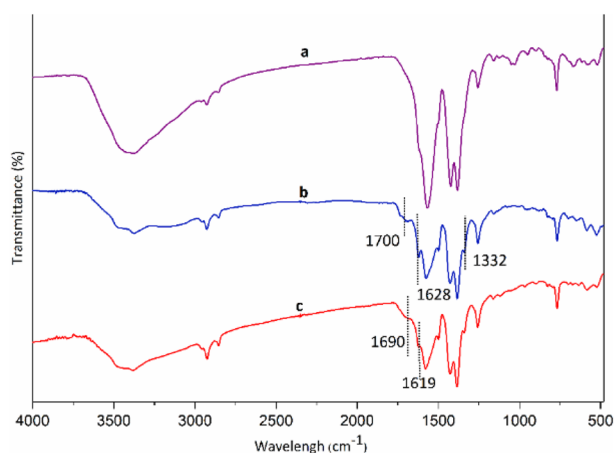


Figure 6. FT-IR spectra of (a) MIL-101(Fe)-NH₂, (b) isatin-Schiff-base-MIL-101(Fe) and (c) Co-isatin-Schiff-base-MIL-101(Fe).

Sample	$S_{\text{BET}}^{\text{a}}$ ($\text{m}^2 \text{g}^{-1}$)	$V_{\text{total}}^{\text{b}}$ ($\text{cm}^3 \text{g}^{-1}$)
MIL-101(Fe)-NH ₂	1810	1.08
Co-isatin-Schiff-base-MIL-101(Fe)	295	0.25

Table 1. Textural properties of pure MIL-101(Fe)-NH₂ and Co-isatin-Schiff-base-MIL-101(Fe). ^aBET surface area. ^bTotal pore volume.

Synthesis of benz-imidazoles/-oxazoles/-thiazoles from alcohols via TOP catalyzed by Co-isatin-Schiff-base-MIL-101(Fe). 2-Substituted benz-imidazoles/-oxazoles/-thiazoles as significant types of heterocycles, have been broadly documented as structural blocks in the preparation of biological and pharmaceutical compounds (Fig. 9)^{45–47}.

The methods for the synthesis of these heterocyclic compounds consist of the reaction of *o*-phenylenediamine with a variety of reagents. Acids, aldehydes, esters, anhydrides, amides, acyl halides, and nitriles are the common reagents that have been introduced in these methods^{48–50}. However, their synthesis directly from readily available alcohols by TOP is more desirable. In these reactions, aldehydes play as highly active reaction intermediates

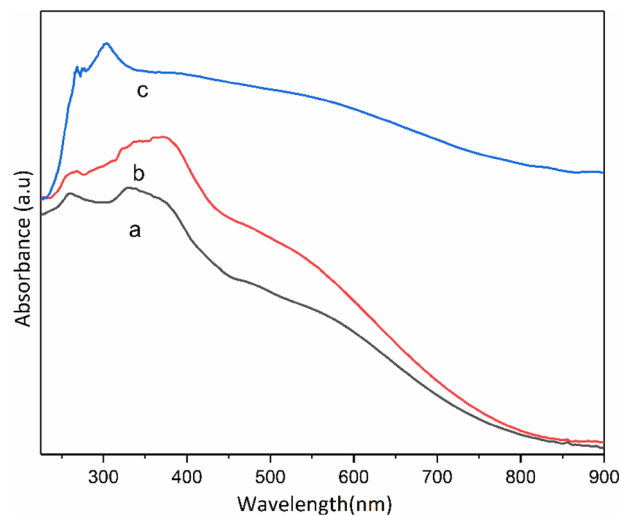


Figure 7. UV-visible absorption spectra of (a) MIL-101(Fe)-NH₂, (b) isatin-Schiff-base-MIL-101(Fe) and (c) Co-isatin-Schiff-base-MIL-101(Fe).

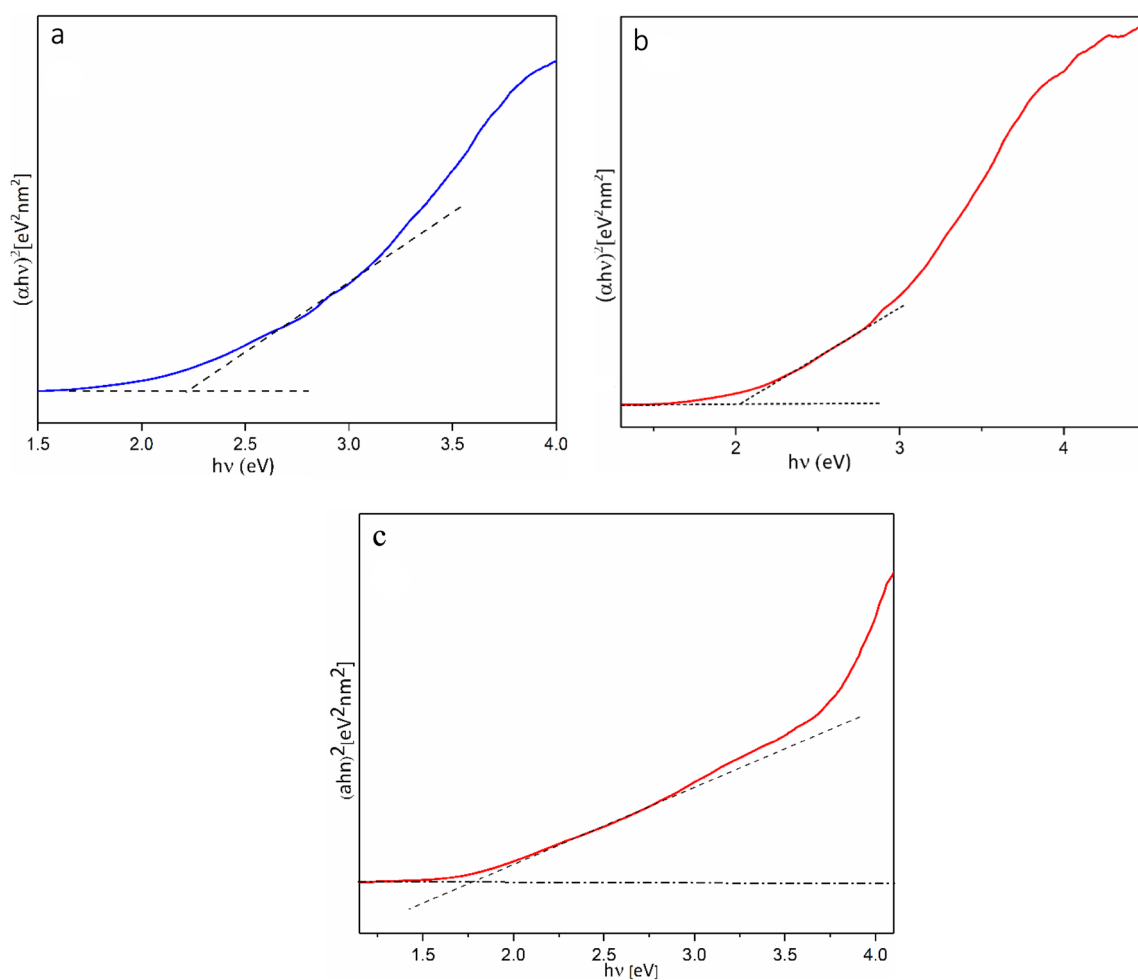


Figure 8. Band gap energy of (a) MIL-101(Fe)-NH₂, (b) isatin-Schiff-base-MIL-101(Fe) and (c) Co-isatin-Schiff-base-MIL-101(Fe).

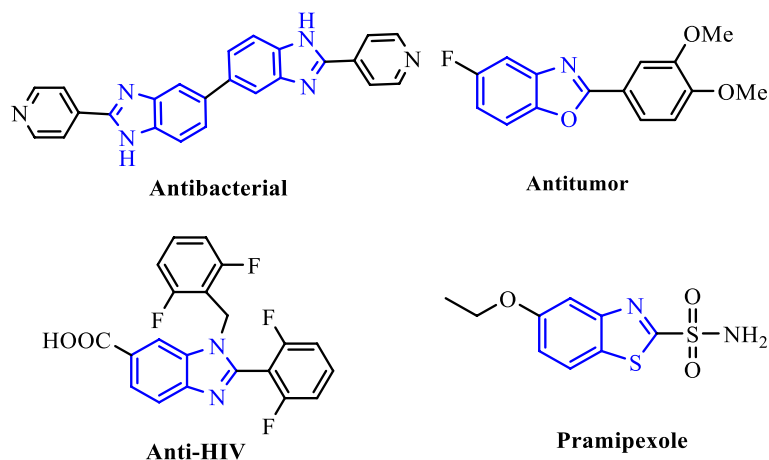


Figure 9. Examples of biologically and pharmaceutically relevant benz-imidazoles/-oxazoles/-thiazoles.

to undergo the subsequent reactions such as condensation with *o*-phenylene diamine, *o*-aminophenol, and/or *o*-aminothiophenol. Numerous materials have been reported to activate these reactions such as porous catalysts, ionic liquids, metal oxides, graphene oxide and MOFs^{51–57}. The reported methods associated with drawbacks such as requiring long reaction time, high temperature, low yields of the products, use of expensive/toxic metals, unrecoverable catalyst and poisonous solvents that may cause environmental pollution^{58–60}.

Therefore, the development of highly efficient alternate methods which proceed under economic and environmental-friendly conditions with energy-saving organic synthetic strategies is desirable. In this paper, we have studied the application of Co-isatin-Schiff-base-MIL-101(Fe) as a heterogeneous multifunctional biophotocatalyst for the synthesis of benz-imidazoles/oxazoles/thiazoles via TOP starting from alcohols. Based on our knowledge, this is the first report of using a bio-photocatalyst for the synthesis of these target molecules.

Initially, the catalyst efficiency for the alcohol photo-oxidation was investigated by selecting benzyl alcohol as a typical compound and the effect of different catalyst loading, solvents, light source and the oxidizing agent was tested for the oxidation of this compound (Table 2). Satisfied results were obtained when 1 mol% of Co-isatin-Schiff-base-MIL-101(Fe) was used in ethanol under sunlight irradiation and air bubbling. The effect of solvents

Entry ^a	Catalyst (mol%)	Oxidant	Solvent	Time (h)	Yield (%)
1	0	Air	EtOH	4	0
2	0.4	Air	EtOH	5	73
3	0.7	Air	EtOH	4	85
4	1	Air	EtOH	4	90
5	1	Air	THF	4	60
6	1	Air	Toluene	4	65
7	1	Air	H ₂ O	5	45
8	1	Air	CH ₃ CN	6	86
9	1	Air	DMF	5	70
10	1	Air	–	4	55
11 ^b	1	Air	EtOH	4	85
12 ^c	1	Air	EtOH	4	70
13 ^d	1	Air	EtOH	8	20
14 ^e	1	–	EtOH	6	0
15	1	O ₂	EtOH	5	92
16 ^f	1	H ₂ O ₂	EtOH	4	30
17 ^f	1	TBHP	EtOH	4	35
18 ^e	1	–	EtOH	4	0

Table 2. Optimization of photo-oxidation of benzyl alcohol to benzaldehyde. ^aReaction conditions: benzyl alcohol (1 mmol), EtOH (6 mL), catalyst (1 mol%, except in entry 1), at ~ 30 °C, under air bubbling (except in entries 14–18) and sunlight irradiation (except in entries 11–13). ^bBlue LED visible light irradiation. ^cRoom light. ^dWithout irradiation (dark). ^eUnder N₂ atmosphere. ^fTBHP and H₂O₂ (1 mmol).

with different polarities on the progress of the reaction was investigated (Table 2, entries 4–10). Low yield of the product under solvent-free conditions (Table 2, entry 10) showed the importance of the solvent for transferring the substrates into the active sites of the catalyst. The lowest yield was obtained in water (Table 2, entry 7) among other organic solvents and the highest yield was observed in ethanol (Table 2, entry 4). The increase in the efficiency of the catalytic process in ethanol can be due to the greater solubility of substances in ethanol and subsequently the easier transfer of substances to the MOF pores and as a result faster interaction with the active catalytic sites. Solvents such as DMF and THF can be coordinated to the active sites of the MOF catalyst and so decrease its catalytic efficiency. The model reaction proceeded with low yields in the presence of H₂O₂ or TBHP (Table 2, entries 16 and 17) probably due to the restricted access to the active sites of the catalyst and their different mechanism pathways. To find the effect of the light on the progress of the reaction, the model reaction was also studied under dark reaction conditions and benzaldehyde was obtained in an insignificant amount after 8 h (Table 2, entry 13). When a similar reaction was performed under N₂ atmosphere, any conversion of benzyl alcohol was not observed (Table 2, entry 18).

To examine the generality of this photo-oxidation method, the reaction of a variety of alcohols was performed using optimized reaction conditions. As shown in Table 3, selective photo-oxidation of primary and secondary benzyl alcohols occurred and the corresponding carbonyl compounds were obtained in 78–90% yields without any overoxidation (entries 1–8). Furfuryl alcohol, as a famous challenging heteroaromatic alcohol and cinnamyl alcohol, containing a conjugated double bond, underwent selective photo-oxidation to furfural and cinnamaldehyde, respectively (Table 3, entries 9 and 10). Aliphatic alcohols exhibited less activity using the present photo-oxidation method (Table 3, entries 11–14).

With successful photo-oxidation of alcohols, in the next part, the efficiency of Co-isatin-Schiff-base-MIL-101(Fe) was investigated in the synthesis of benzimidazoles from alcohols via TOP. The reaction of benzyl alcohol and *o*-phenylenediamine was chosen as a typical reaction to discover the best catalyst loading and the appropriate solvent (Table 4). The best result was achieved using 1.2 mol% of the catalyst in ethanol (Table 4, entry 6).

The reactions of a number of benzyl alcohols containing electron-withdrawing or -releasing groups and *o*-substituted anilines catalyzed by Co-isatin-Schiff-base-MIL-101(Fe) were performed under the optimum reaction conditions (Table 5). As depicted in Table 5, benzyl alcohols and *o*-substituted anilines (*o*-phenylene diamine, *o*-aminophenol, and/or *o*-aminothiophenol) underwent the TOP reaction with high efficiency to give benzimidazoles/-oxazoles/-thiazoles, respectively, in good to high yields. The functional groups (methyl, nitro, and chloride) in the benzyl alcohol stayed with no change in the TOP reaction.

To understand the role of Co-isatin-Schiff-base-MIL-101(Fe) in this reaction, the photocatalytic efficiency of cobalt-free precursors of the catalyst [MIL-101(Fe)-NH₂ and isatin-Schiff-base-MIL-101(Fe)] and Co-isatin-Schiff-base were examined in the model reaction for the synthesis of benzimidazole under the optimized reaction conditions (Table 6, entries 1–4). Comparison of the obtained results with those of Co-isatin-Schiff-base-MIL-101(Fe) showed a significant decrease in the catalytic efficiency of cobalt-free precursors and Co-isatin-Schiff-base. Similar reactions in the presence of FeCl₃·6H₂O or Co(OAc)₂·4H₂O did not show any significant progress (Table 6, entries 5 and 6). These experiments obviously revealed that the photocatalytic efficiency of Co-isatin-Schiff-base-MIL-101(Fe) is related primarily to the synergetic effect of Fe–O cluster and Co-Schiff-base. The presence of the synergetic effect could be clarified by a significant decrease in the band gap energy and an increase in the fluorescence emission of MIL-101(Fe) after functionalization with cobalt Schiff-base complex according to DRS analysis (Fig. 8) and fluorescence spectrophotometry (Fig. 10), respectively. In order to indicate the importance of sunlight irradiation and also air in the progress of the reaction, two more experiments were carried out. Under dark conditions, only a trace amount of benzimidazole was obtained (Table 6, entry 7) and benzyl alcohol remained intact in the presence of N₂ atmosphere (Table 6, entry 8). Additionally, when benzaldehyde was used instead of benzyl alcohol as the starting material, the desired product was produced in shorter time (Table 6, entry 9). The effect of sunlight irradiation and also air in the progress of the reaction starting from benzaldehyde was studied. Under dark conditions or in the presence of N₂ atmosphere, a low yield of benzimidazole was obtained (Table 6, entries 10 and 11). These experiments clearly indicate that the catalytic oxidation reaction takes place in two key steps: (1) selective photo-oxidation of benzyl alcohol to benzaldehyde and (2) dehydrogenation reaction, which takes place after condensation reaction of benzaldehyde with *o*-phenylenediamine.

The electron paramagnetic resonance (EPR) measurements were recorded to detect reactive oxygen species (ROS) formed during the photocatalytic step. By using 2,2,6,6-tetramethylpiperidine (TEMP), as the singlet oxygen (¹O₂) detection agent, a strong 1:1:1 triplet signal was depicted (Fig. 11a), proving ¹O₂ formation over Co-isatin-Schiff-base-MIL-101(Fe) under the optimum conditions. When 5,5-dimethyl-1-pyrroline *N*-oxide (DMPO) as a superoxide radical anion (O₂^{•−}) detection agent was used, strong signals appeared (Fig. 11b), which indicates that O₂^{•−} species were also formed during the photocatalytic reaction.

Based on our observation and also the postulated mechanisms in the literature^{28,29,34,62}, a mechanism is proposed in Fig. 12. When Co-isatin-Schiff-base-MIL-101(Fe) is irradiated, the singlet excited state of MOF and the holes were produced. The excited electrons in the valence band reduces O₂ to form O₂^{•−} by single electron transfer (SET). Moreover, singlet excited state of MOF can be converted to triplet excited state by intersystem crossing. The produced triplet excited state activates oxygen to ¹O₂ through energy transfer process. The holes (h⁺) oxidize benzyl alcohol into benzyl alcohol⁺, which further reacted with formed O₂^{•−} and ¹O₂ to produce benzaldehyde. In the next step, the Lewis acidic iron and cobalt sites in Co-isatin-Schiff-base-MIL-101(Fe) catalyze the condensation of the as-formed aldehyde and *o*-phenylenediamine to generate the cyclic compound, which is more oxidized to benzimidazole. To determine the active species involved in the catalytic cycle, the photocatalytic reaction was individually investigated using some famous scavengers. In the presence of *p*-benzoquinone (BQ), NaN₃ and ammonium oxalate, the photocatalytic efficiency of the MOF was decreased obviously. The above results indicate that O₂^{•−}, ¹O₂ and h⁺ are the principal oxidants in the photocatalytic procedure.

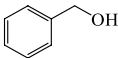
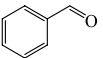
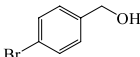
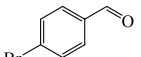
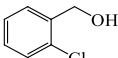
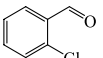
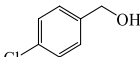
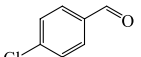
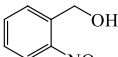
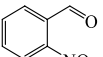
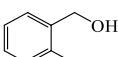
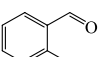
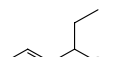
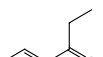
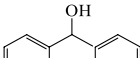
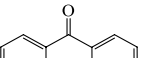
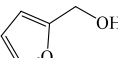
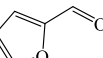
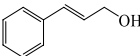
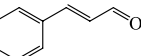
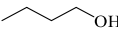
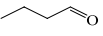
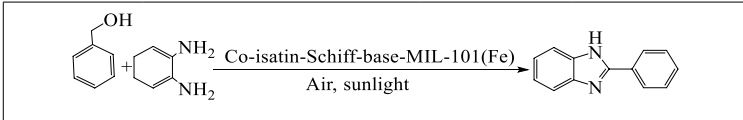
Entry ^a	Alcohol	Product	Time (h)	Yield (%)
1			4	90
2			5	88
3			6	85
4			6	87
5			6	87
6			7	86
7			6	78
8			5.5	80
9			7	85
10			7	75
11			7	73
12			8	53
13			8	44
14			8	37

Table 3. Photo-oxidation of alcohols catalyzed by Co-isatin-Schiff-base-MIL-101(Fe) in the presence of air under sunlight irradiation. ^aReaction conditions: alcohol (1 mmol), EtOH (6 mL), catalyst (1 mol%), ~30 °C, under air bubbling and sunlight conditions. Turnover number [TON (mol of the product per mol of the catalyst)] = 37–90, turnover frequency [TOF (TON/time)] = 4.6–22.5 h⁻¹.



Entry	Catalyst (mol %)	Solvent	Yield (%)
1	0	EtOH	0
2	0.2	EtOH	52
3	0.4	EtOH	66
4	0.7	EtOH	72
5	1	EtOH	83
6	1.2	EtOH	90
7	1.5	EtOH	90
8	1.2	THF	77
9	1.2	Toluene	74
10	1.2	H ₂ O	29
11	1.2	DMF	78
12	1.2	CH ₃ CN	85

Table 4. Optimization of the reaction conditions for the synthesis of benzimidazoles from alcohols via TOP catalyzed by Co-isatin-Schiff-base-MIL-101(Fe). Reaction conditions: *o*-phenylenediamine (1 mmol), benzyl alcohol (1 mmol), solvent (6 mL), 8 h, air bubbling and sunlight irradiation, ~30 °C.

The reusability of Co-isatin-Schiff-base-MIL-101(Fe) was studied in the model reaction of the synthesis of benzimidazole from alcohol via TOP. For this purpose, after completion of the reaction, ethanol (10 mL) was added to the mixture and the reaction mixture was centrifuged to separate the catalyst. The recovered catalyst after washing with ethanol was reused in five consecutive runs in the model reaction with insignificant decrease in the catalytic activity (Fig. 13). The FT-IR spectrum, and TEM image of the reused catalyst indicate that the structure of the catalyst preserved after five times recycling (Fig. 14).

A classical hot-filtration examination was employed to explore whether Co-isatin-Schiff-base-MIL-101(Fe) works as a heterogeneous bio-photocatalyst or releases cobalt ions. Towards this point, synthesis of benzimidazole directly from alcohol was investigated under the optimized reaction conditions. In half time of the reaction (4 h), the reaction mixture was centrifuged to separate the catalyst. Then the reaction was allowed to be continued for an additional 4 h. Any progress in the reaction was not observed by increasing the reaction time (Fig. 15b). The nature of the catalytic mode (homogeneous or heterogeneous) was surveyed using a poisoning test. For this purpose, the model reaction of the synthesis of benzimidazole was performed in the presence of S₈ (0.05 g) to kidnap the possible released cobalt species. No changes in the reaction course compared to normal one (Fig. 15a) were identified, which revealed the absence of the leached homogeneous cobalt particles in the solution (Fig. 15c).

Tandem photo-oxidation/Knoevenagel condensation reaction catalyzed by Co-isatin-Schiff-base-MIL-101(Fe). The results of benzimidazole synthesis from alcohols via TOP, encouraged us to investigate the photocatalytic performance of Co-isatin-Schiff-base-MIL-101(Fe) in the tandem photo-oxidation/Knoevenagel condensation reaction of alcohols and malononitrile. For this purpose, the reaction of benzyl alcohol and malononitrile under sunlight irradiation at ~30 °C was selected as a model reaction to optimize the reaction conditions such as the amount of the catalyst and solvent (Table 7). 1.5 mol% of Co-isatin-Schiff-base-MIL-101(Fe) was the most effective amount of the catalyst (Table 7, entry 3). Some solvents such as EtOH, THF, toluene, H₂O, CH₃CN and also solvent-free conditions were tested (Table 7, entries 3 and 5–10) and found that the reaction is efficiently promoted in EtOH compared to other solvents (Table 7, entry 3). To show the effect of the irradiation on the progress of the reaction, a similar reaction in the absence of any light and air was also studied and any conversion of the starting material was not detected (Table 7, entry 11).

Having the optimized reaction conditions, the photo-oxidation/Knoevenagel condensation reaction of various alcohols were examined (Table 8). As the results of Table 8 show, benzyl alcohols containing different substituents underwent the photo-oxidation/Knoevenagel condensation reaction with malononitrile and produced the desired products in good to high yields (Table 8, entries 1–8). The reaction of ethyl cyanoacetate as a compound with active methylene and alcohol proceeded well under the same reaction conditions (Table 8, entries 9 and 10).

Furthermore, we have found that furfuryl alcohol (Fig. 16) was suitable substrate for photo-oxidation/Knoevenagel reaction under the optimal conditions, and produced the desired Knoevenagel condensation product in 75% yield.

To find the role of Co-isatin-Schiff-base-MIL-101(Fe) in the photo-oxidation/Knoevenagel reaction, the model reaction was studied in the presence of cobalt-free precursors of the catalyst [MIL-101(Fe)-NH₂ and isatin-Schiff-base-MIL-101(Fe)] or Co-isatin-Schiff-base (Table 9, entries 1–4). A significant decrease in the catalytic efficiency of cobalt-free precursors and Co-isatin-Schiff-base was observed compared with Co-isatin-Schiff-base-MIL-101(Fe). The importance of sunlight irradiation and air in the reaction was also investigated.

Entry	Benzyl alcohol	X	Product	Yield (%)	Obtained M.P. (°C)	Reported M.P. (°C) ^{Ref}
1		NH		90	288–290	290–294 ³⁰
2		NH		78	288–290	289–291 ³⁰
3		NH		83	262–264	263–265 ³⁰
4		NH		80	308–310	309–310 ³⁰
5		O		83	198–200	201–203 ³⁰
6		O		75	209–211	209–211 ³⁰
7		O		80	90–92	88–90 ⁵⁸
8		O		77	262–264	261–262 ⁶⁰
9		S		80	109–110	110–112 ³⁰
10		S		73	113–115	114–116 ³⁰
11		S		76	84–86	85–87 ⁶¹
12		S		74	227–228	226–227 ⁶¹

Table 5. Photo-induced synthesis of different benz-imidazoles/-oxazoles/-thiazoles catalyzed by Co-isatin-Schiff-base-MIL-101(Fe) from alcohols via TOP. Reaction conditions: *o*-substituted anilines (1 mmol), benzyl alcohol (1 mmol), EtOH (6 mL), catalyst (1.2 mol%), 8 h, air bubbling, sunlight irradiation and ~ 30 °C. The products were identified by NMR spectroscopy (see supplementary information file). TON (mol of the product per mol of the catalyst = 61–75), TOF (TON/time) = 7.6–9.4 h.

The product was obtained only in a trace amount under dark conditions (Table 9, entry 5) and alcohol remained intact in the presence of N₂ atmosphere (Table 9, entry 6).

When benzaldehyde was used instead of benzyl alcohol as the starting material, the target product was produced more rapidly (Table 9, Entries 7–9). These experiments clearly indicate that the reaction using Co-isatin-Schiff-base-MIL-101(Fe) actually takes place in two key steps: step (1) photo-oxidation of benzyl alcohol to benzaldehyde and step (2) Knoevenagel condensation reaction between the *in situ* formed benzaldehyde and malononitrile. Additional control experiments reveal that Co-isatin-Schiff-base-MIL-101(Fe) act as a photosensitizer which contains Fe (III) and Co (II) counterparts as typical Lewis acidic sites and worked well synergistically.

Entry	Catalyst	Light irradiation	Yield (%)
1	MIL-101(Fe)-NH ₂	Sunlight	40
2	Isatin-Schiff-base-MIL-101(Fe)	Sunlight	50
3 ^a	Co-isatin-Schiff-base	Sunlight	Trace
4	Co-isatin-Schiff-base-MIL-101(Fe)	Sunlight	90
5	FeCl ₃ ·6H ₂ O	Sunlight	Trace
6	Co(OAc) ₂ ·4H ₂ O	Sunlight	Trace
7	Co-isatin-Schiff-base-MIL-101(Fe)	Dark	Trace
8 ^b	Co-isatin-Schiff-base-MIL-101(Fe)	Sunlight	Trace
9 ^c	Co-isatin-Schiff-base-MIL-101(Fe)	Sunlight	90
10 ^c	Co-isatin-Schiff-base-MIL-101(Fe)	Dark	25
11 ^{c,b}	Co-isatin-Schiff-base-MIL-101(Fe)	Sunlight	25

Table 6. Effect of different catalytic species or conditions on the synthesis of benzimidazole. Reaction conditions: o-phenylenaniline (1 mmol), benzyl alcohol (1 mmol, except in entries 9–11), EtOH (6 mL), catalyst (5.3 mg), 8 h (except in entry 9). ^aCo-isatin-Schiff-base (isatin-Schiff-base was prepared by the reaction of isatin and aniline). ^bUnder N₂ atmosphere. ^cBenzaldehyde (1 mmol), 4 h.

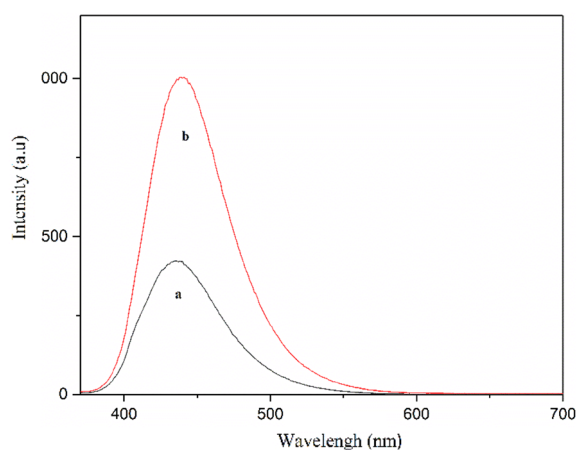


Figure 10. Emission spectra of (a) MIL-101(Fe)-NH₂ and (b) Co-isatin-Schiff-base-MIL-101(Fe).

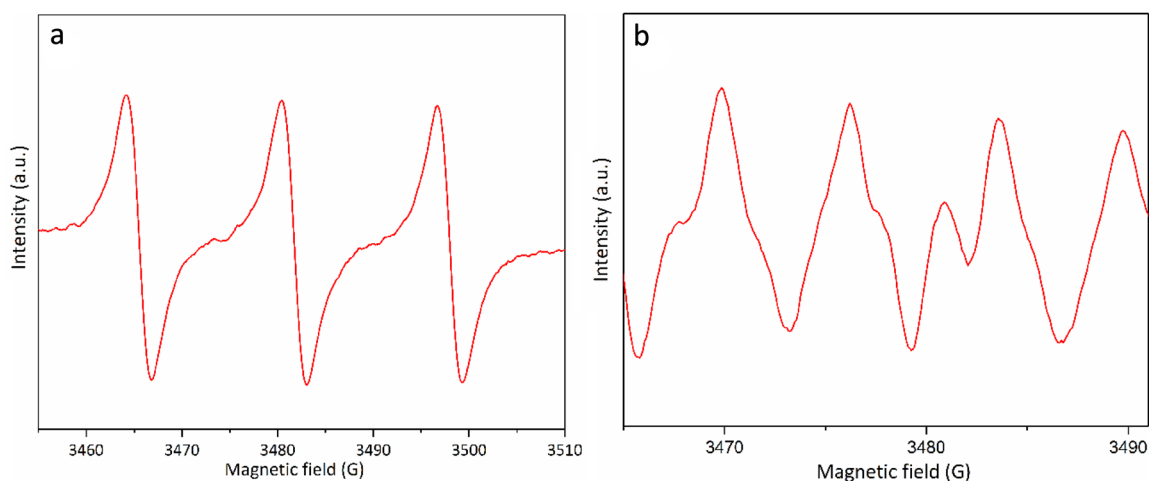


Figure 11. (a) EPR spectra for ¹O₂ detection by TEMP and (b) EPR detection of O₂⁻ by DMPO.

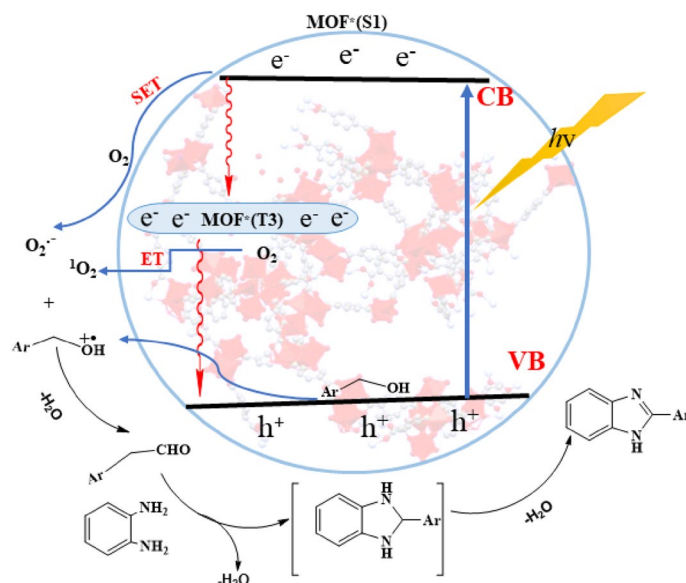


Figure 12. Proposed mechanism for the synthesis of 2-phenylbenzimidazole from *o*-phenylenediamine and alcohol over Co-isatin-Schiff-base-MIL-101(Fe).

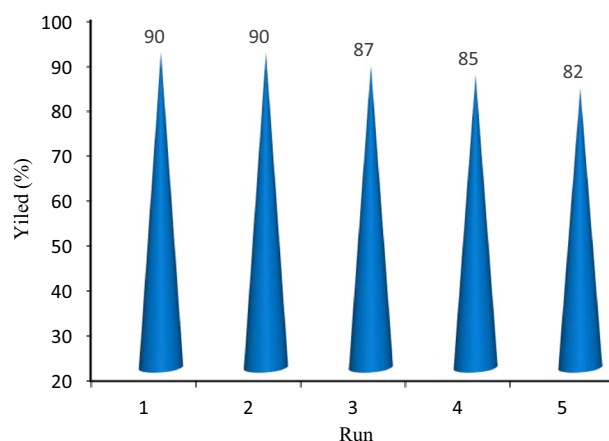


Figure 13. Reusability of the Co-isatin-Schiff-base-MIL-101(Fe) during synthesis of benzimidazole.

Hence, according to the control experiments, our observation above and literature survey^{32–34}, a possible mechanism for the TOP photo-oxidation/Knoevenagel condensation reaction can be proposed (Fig. 17). The generated hole (h^+) rapidly oxidizes the benzyl alcohol to create radical cation species (A) as the intermediates, which can consequently react with ROS ($O_2^{\cdot-}$ and 1O_2) to produce the corresponding aldehyde (B). Next, Co-isatin-Schiff-base-MIL-101(Fe) including the Lewis acidic sites (Fe^{3+} and Co^{2+}) activates the in situ-produced aldehyde and malonitrile for a nucleophilic addition via Knoevenagel coupling reaction toward the formation of the final product (C).

Finally, the photocatalytic efficiency of the present catalyst was compared with the MOF-based photocatalysts in the benzimidazole synthesis and Knoevenagel condensation starting from alcohols via TOP reported in the literature (Table 10). As represented in Table 10, Co-isatin-Schiff-base-MIL-101(Fe) exhibits the most effective photocatalytic activity for both benzimidazole synthesis and Knoevenagel condensation under sunlight irradiation. The reported methods suffer from drawbacks such as using toxic solvents, high temperature, requiring UV irradiation, prolong reaction time, high catalyst loading and expensive metals. It is worth to mention that because of the high energy of UV photons, which causes the chemical degradation or side reactions, there is a limitation in using UV light irradiation.

Photocatalytic antibacterial efficiency of Co-isatin-Schiff-base-MIL-101(Fe). Bacterial pollution intimidates the nutrition, water and community health. Antibiotics are the most famous antibacterial agents for medical treatment of infections caused by bacteria^{65,66}. Using a great amount of antibiotics makes bacteria to be resistant towards medicines and so would be lethal for the patients^{67,68}. Therefore, introduction of novel

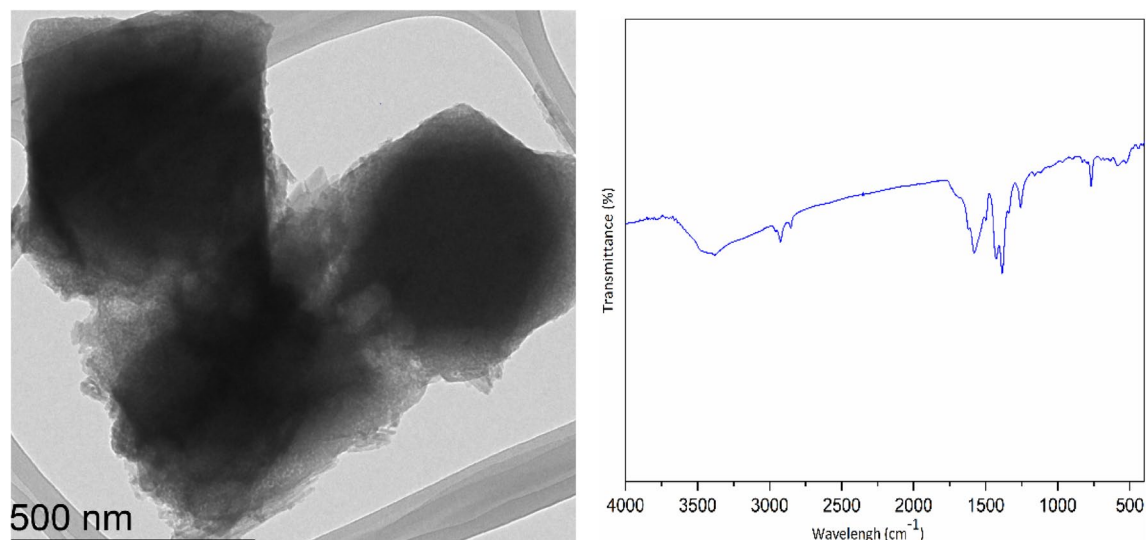


Figure 14. TEM image and FT-IR spectrum of Co-isatin-Schiff-base-MIL-101(Fe) after five times reuse in the synthesis of benzimidazole.

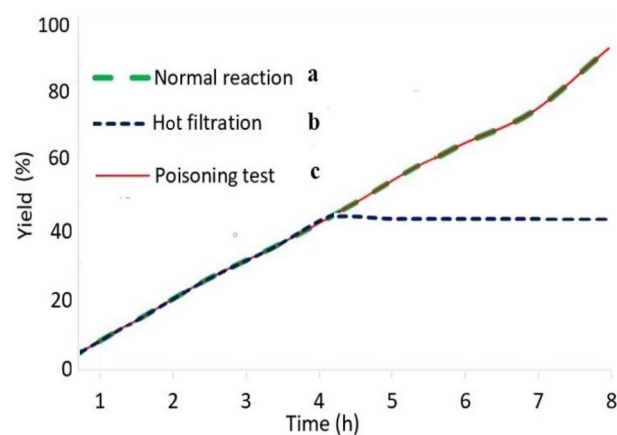
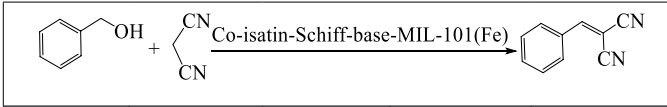


Figure 15. Synthesis of benzimidazole starting from alcohol using Co-isatin-Schiff-base-MIL-101(Fe) as a photocatalyst: (a) normal reaction, (b) employing a hot filtration protocol and (c) using S_8 as a poison for the catalyst.

and efficient antibacterial agents, which are different from antibiotics is demanded⁶⁹. Nowadays, due to the harmless, efficient, and extensive disinfection influence of semiconductors, they are widely used as antibacterial agents in photocatalytic process. During this process, in the semiconductors, electrons are excited by visible light irradiation and some holes are generated. Then reactive oxygen radicals (HO^\bullet , $O_2^{\bullet-}$) are formed by the reaction of electrons and holes with water and oxygen, which destruct cell walls of bacteria and thus disable the microorganisms^{70,71}. MOFs as semiconductors are known as a new generation of antibacterial agents. They have enormous surface area, highly-distributed active sites, tunable porous size, and high biocompatibility and biodegradability^{72,73}.

Herein, the photocatalytic antibacterial activity of Co-isatin-Schiff-base-MIL-101(Fe) against *E. coli*, *S. aureus* and *S. pyogenes* was studied under sunlight illumination. The results showed that almost all bacteria were inactivated after 2 h irradiation in the presence of MOF as a bio-photo-antibacterial agent, with the antibacterial efficiency of 99.57%, 99.85% and 99.48%, for *E. coli*, *S. aureus* and *S. pyogenes*, respectively. The negligible decreasing in the bacterial density treated with photocatalyst in the dark or without Co-isatin-Schiff-base-MIL-101(Fe) at light conditions indicates that both light irradiation and photocatalyst are necessary for the efficient antibacterial activity. Moreover, minimal inhibitory concentration (MIC) and minimal bactericidal concentration (MBC) values for *E. coli* and *S. aureus* are the same and are higher in the case of *S. pyogenes* (Table 11).



Entry ^a	Catalyst	Solvent	Time (h)	Yield (%)
1	0.5	EtOH	8	67
2	0.9	EtOH	8	78
3	1.5	EtOH	5	88
4	2	EtOH	5	88
5	1.5	THF	5	50
6	1.5	Toluene	5	43
7	1.5	H ₂ O	5	35
8	1.5	CH ₃ CN	5	82
9	0	EtOH	5	trace
10	1.5	-	8	47
11 ^{b,c}	1.5	EtOH	10	0

Table 7. Tandem one-pot photo-oxidation/Knoevenagel condensation reaction of alcohols catalyzed by Co-isatin-Schiff-base-MIL-101(Fe). ^aReaction conditions: benzyl alcohol (1 mmol), malononitrile (1 mmol), solvent (6 mL), catalyst (1.5 mol%), air bubbling, sunlight irradiation (except in entry 11), ~ 30 °C. ^bDark conditions. ^cUnder N₂ atmosphere.

Conclusion

In conclusion, a metal–organic framework functionalized with cobalt-complex [Co-isatin-Schiff-base-MIL-101(Fe)] as a heterogeneous multifunctional bio-photocatalyst for the synthesis of benz-imidazoles/-oxazoles/-thiazoles, and benzylidene malononitrile by tandem oxidation process starting from readily available alcohols is introduced. In this method, photo-oxidation of alcohols and cyclocondensation of the *in-situ* formed aldehydes with *o*-substituted aniline (*o*-phenylenediamine/*o*-aminophenol/*o*-aminothiophenol) or malononitrile affords benz-imidazoles/-oxazoles/-thiazoles, or benzylidene malononitrile, respectively, in one-pot operation in good to high yields. Co-isatin-Schiff-base-MIL-101(Fe) acts both as a bio-photocatalyst to produce reactive ¹O₂, O₂^{•-}, and a Lewis acid to catalyze the reaction of the *in-situ* formed aldehydes with *o*-substituted anilines or malononitrile. A significant decrease in the band gap energy and an increase in the characteristic emission of MIL-101(Fe) after functionalization with cobalt Schiff-base according to DRS analysis and fluorescence spectroscopy, respectively, indicate that the photocatalytic efficiency of Co-isatin-Schiff-base-MIL-101(Fe) is related primarily to the synergistic effect of Fe–O cluster and Co-Schiff-base. EPR results obviously point out that Co-isatin-Schiff-base-MIL-101(Fe) is capable of generating ¹O₂ and O₂^{•-} as active oxygen species under visible light irradiation. The use of sunlight and air as abundant and cheap sources without needing any specific chemical oxidizing agent, using low loading of a reusable bio-photocatalyst in ethanol as an environmentally friendly solvent, and easy separation of the obtained products are the advantages of this method. Moreover, Co-isatin-Schiff-base-MIL-101(Fe) exhibits outstanding sunlight-induced photocatalytic antibacterial activity for the inactivation of three kinds of bacteria. Based on our knowledge, this is the first report of using a bio-photocatalyst for the synthesis of the target molecules.

X = CN, CO₂Et

Entry	R	X	Product	Time (h)	Yield (%)	Obtained M.P. (°C)	Reported M.P. (°C) ^{Ref}
1	H	CN		5	88	81–83	80–82 ⁶³
2	CH ₃	CN		8	87	131–133	130 ⁶⁴
3	OCH ₃	CN		8	88	113–114	111–113 ⁶³
4	Br	CN		6	85	153–155	152–154 ⁶³
5	Cl	CN		6.5	83	163–165	162–163 ⁶³
6	2-Cl	CN		8	80	82–84	80–82 ⁶³
7	NO ₂	CN		6	84	158–160	156–158 ⁶³
8	OH	CN		8	73	183–185	180–182 ⁶⁴
9	H	CO ₂ Et		8	67	51–52	49–51 ⁶³
10	OCH ₃	CO ₂ Et		7	65	78–80	78–80 ⁶³

Table 8. TOP photo-oxidation/Knoevenagel condensation reaction of alcohols catalyzed by Co-isatin-Schiff-base-MIL-101(Fe). Reaction conditions: benzyl alcohol (1 mmol), malononitrile (1 mmol), EtOH (6 mL), catalyst (1.5 mol%), air bubbling, sunlight irradiation, ~ 30 °C. Structure of the products were identified by NMR spectroscopy (see supporting information). TON (mol of the product per mol of the catalyst = 43.3–58.6), TOF (TON/time) = 5.6–11.7 h.

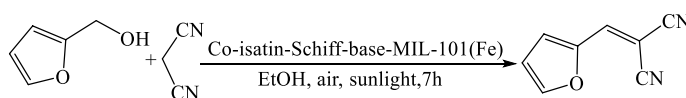


Figure 16. Synthesis of (2-furylmethylene) malononitrile from furfuryl alcohol.

Entry	Catalyst	Light irradiation	Time (h)	Yield (%)
1	MIL-101(Fe)-NH ₂	+	5	28
2	Isatin-Schiff-base-MIL-101(Fe)	+	5	38
3 ^a	Co-isatin-Schiff-base	+	5	trace
4	Co-isatin-Schiff-base-MIL-101(Fe)	+	5	88
5	Co-isatin-Schiff-base-MIL-101(Fe)	-	5	Trace
6 ^b	Co-isatin-Schiff-base-MIL-101(Fe)	+	5	0
7 ^c	Co-isatin-Schiff-base-MIL-101(Fe)	+	1.5	92
8 ^c	Co-isatin-Schiff-base-MIL-101(Fe)	-	1.5	92
9 ^{b,c}	Co-isatin-Schiff-base-MIL-101(Fe)	+	1.5	92

Table 9. Effect of different catalytic species or conditions on tandem one-pot photo-oxidation/Knoevenagel. Reaction conditions: benzyl alcohol (1 mmol, except in entries 8–10), malononitrile (1 mmol), EtOH (6 mL), catalyst (7 mg), air bubbling, sunlight irradiation, ~ 30 °C. ^aCo-isatin-Schiff-base (isatin-Schiff-base was prepared by the reaction of isatin and aniline). ^bUnder N₂ atmosphere. ^cBenzaldehyde (1 mmol).

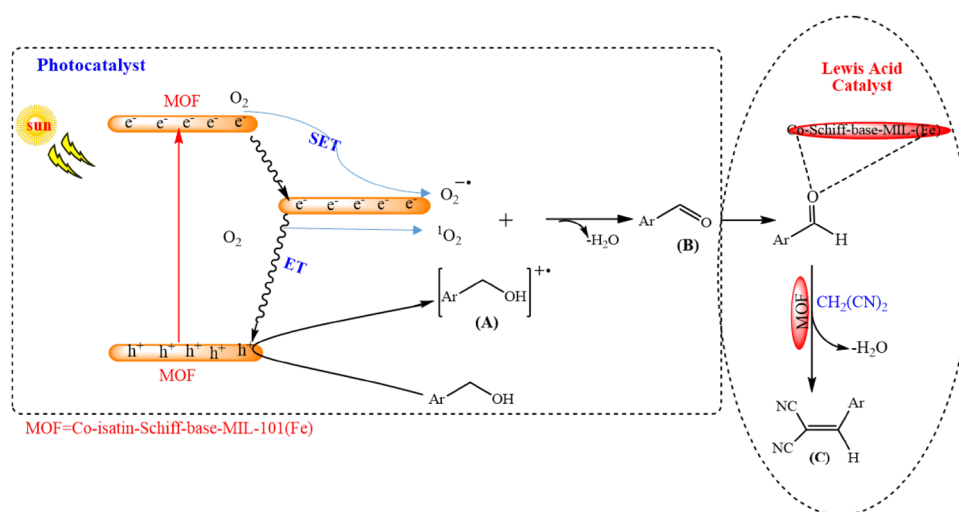


Figure 17. Proposed mechanism for the TOP photo-oxidation/Knoevenagel condensation reaction of alcohols catalyzed by Co-isatin-Schiff-base-MIL-101(Fe).

Entry ^{ref}	Catalyst	Product	Reaction conditions	Time (h)	Isolated yield (%)
1 ³⁰	W-ZnO@NH ₂ -CBB ^a (20 mg)	Benzimidazole	EtOH, air, UV-Vis	2	88–99
2 ²⁸	Au/MIL-101 (Fe) (100 mg)	Benzimidazole	EtOH, O ₂ , visible light	12	49.5–95.1
3 ²⁹	MIL-100 (Fe) (100 mg)	Benzimidazole	CH ₃ CN, O ₂ , visible light (300 W Xe)	10	38–96
4 ³¹	Pt-MIL-101(Fe) (20 mg)	Benzimidazole	CH ₃ CN, N ₂ , visible light (300 W Xe)	24	63.6–87
5 ^{this work}	Co-isatin-Schiff-base-MIL-101(Fe) (5.3 mg)	Benzimidazole	EtOH, air, sunlight irradiation (~30 °C)	8	73–90
6 ³²	Zr-MOF-NH ₂ (1000 mg)	Benzylidenemalononitrile	<i>p</i> -xylene, 90 °C, UV-light irradiation	48	91
7 ³³	MIL-101 (Fe)-NH ₂ (200 mg)	Benzylidenemalononitrile	C ₆ H ₅ CF ₃ /CH ₃ CN, O ₂ , visible light (300 W Xe)	40	20–76
8 ³⁴	PorphCat-Fe ^b (40 mg)	Benzylidenemalononitrile	CH ₃ CN, visible light (~34 °C), O ₂ (1 atm)	24	91
9 ^{this work}	Co-isatin-Schiff-base-MIL-101(Fe) (7 mg)	Benzylidenemalononitrile	EtOH, air, sunlight irradiation (~30 °C)	4–8	65–88

Table 10. Comparison of photocatalytic efficiency of Co-isatin-Schiff-base-MIL-101(Fe) with some reported MOFs-based photocatalysts for benzimidazole and benzylidenemalononitrile synthesis via one-pot TOP started from alcohols. ^aCBB = Coomassie brilliant blue, ^bporphyrin catecholate iron-based MOF.

Bacteria	MIC ^a	MBC ^a
<i>E. coli</i>	250	500
<i>S. aureus</i>	250	500
<i>S. pyogenes</i>	500	1000

Table 11. The antibacterial test results of Co-isatin-Schiff-base-MIL-101(Fe) for different bacterial strains: *E. coli*, *S. aureus* and *S. pyogenes* under sunlight irradiation. ^aMinimal inhibitory concentration (MIC) and minimal bactericidal concentration (MBC) values were reported as $\mu\text{g mL}^{-1}$.

Data availability

All data generated or analysed during this study are included in this published article (and its Supplementary Information files).

Received: 7 December 2022; Accepted: 24 March 2023

Published online: 29 March 2023

References

- Shahsavari, A. & Akbari, M. Potential of solar energy in developing countries for reducing energy-related emissions. *Renew. Sustain. Energy Rev.* **90**, 275–291 (2018).
- Felipin, F. X. & Fouquet, E. Heterogeneous multifunctional catalysts for tandem processes: An approach toward sustainability. *Chemsuschem* **1**, 718–724 (2008).
- Calmanti, R., Selva, M. & Perosa, A. Tandem Catalysis: One-pot synthesis of cyclic organic carbonates from olefins and carbon dioxide. *Green Chem.* **23**, 1921–1941 (2021).
- Maji, M., Panja, D., Borthakur, I. & Kundu, S. Recent advances in sustainable synthesis of *N*-heterocycles following acceptorless dehydrogenative coupling protocol using alcohols. *Org. Chem. Front.* **8**, 2673–2709 (2021).
- Shaabani, A. *et al.* Chemically functionalized MIL-101-NH₂ with Cobalt (II) tetrasulfophthalocyanine: An efficient catalyst for the aerobic oxidation of alcohols and one-pot tandem conversion of alcohols to propargylamines. *J. Taiwan Inst. Chem. Eng.* **126**, 211–222 (2021).
- Hoffmann, N. Photochemical reactions as key steps in organic synthesis. *Chem. Rev.* **108**, 1052–1103 (2008).
- Deng, X., Li, Z. & Garcia, H. Visible light induced organic transformations using metal-organic-frameworks (MOFs). *Eur. J. Chem.* **23**, 11189–11209 (2017).
- Protti, S. & Fagnoni, M. The sunny side of chemistry: Green synthesis by solar light. *Photochem. Photobiol. Sci.* **8**, 1499–1516 (2009).
- Pavanello, A. *et al.* Biomimetic photooxidation of noscaphine sensitized by a riboflavin derivative in water: The combined role of natural dyes and solar light in environmental remediation. *Photochem. Photobiol.* **229**, 112415–112423 (2022).
- Sharma, M. *et al.* Solar light assisted degradation of dyes and adsorption of heavy metal ions from water by CuO–ZnO tetrapodal hybrid nanocomposite mater. *Today Chem.* **17**, 100336–100348 (2020).
- Gopinath, C. S. & Nalajala, N. A scalable and thin film approach for solar hydrogen generation: A review on enhanced photocatalytic water splitting. *J. Mater. Chem. A* **9**, 1353–1371 (2021).
- Fujishima, A. & Honda, K. Electrochemical photolysis of water at a semiconductor electrode. *Nature* **238**, 37–38 (1972).
- Qi, K., Cheng, B., Yu, J. & Ho, W. Review on the improvement of the photocatalytic and antibacterial activities of ZnO. *J. Alloys Compd.* **727**, 792–820 (2017).
- Qiu, J. *et al.* Modified metal-organic frameworks as photocatalysts. *Appl. Catal. B Environ.* **231**, 317–342 (2018).
- Li, H., Eddaoudi, M., O’Keeffe, M. & Yaghi, O. M. Design and synthesis of an exceptionally stable and highly porous metal-organic framework. *Nature* **402**, 276–279 (1999).
- Kirchon, A., Feng, L., Drake, H. F., Joseph, E. A. & Zhou, H. C. From fundamentals to applications: A toolbox for robust and multifunctional MOF materials. *Chem. Soc. Rev.* **47**, 8611–8638 (2018).
- Hosono, N. & Kitagawa, S. Modular design of porous soft materials via self-organization of metal-organic cages. *Acc. Chem. Res.* **51**, 2437–2446 (2018).
- Huang, C. W. *et al.* Metal-organic frameworks: Preparation and applications in highly efficient heterogeneous photocatalysis. *Sustain. Energy Fuels* **4**, 504–521 (2020).
- Hao, M. & Li, Z. Visible light-initiated synergistic/cascade reactions over metal-organic frameworks. *Sol. RRL.* **5**, 2000454–2000467 (2021).
- Cadiau, A. *et al.* A titanium metal-organic framework with visible-light-responsive photocatalytic activity. *Angew. Chem. Int. Ed.* **59**, 13468–13472 (2020).
- Sun, D. *et al.* Construction of a supported Ru complex on bifunctional MOF-253 for photocatalytic CO₂ reduction under visible light. *Chem. Commun.* **51**, 2645–2648 (2015).
- Xu, C. *et al.* Turning on visible-light photocatalytic C–H oxidation over metal-organic frameworks by introducing metal-to-cluster charge transfer. *J. Am. Chem. Soc.* **141**, 19110–19117 (2019).
- Xu, P. *et al.* A novel heterogeneous catalyst NH₂-MIL-88/PMo 10V₂ for the photocatalytic activity enhancement of benzene hydroxylation. *Catal. Sci. Technol.* **11**, 6507–6515 (2021).
- Xie, D., Wang, S., Li, S., Yang, W. & Feng, Y. S. A two-dimensional Bi-based porphyrin metal-organic framework photocatalyst for white light-driven selective oxidation of sulfides. *Catal. Sci. Technol.* **12**, 3254–3260 (2022).
- Zhang, Y., Huang, C. & Mi, L. Metal-organic frameworks as acid-and/or base-functionalized catalysts for tandem reactions. *Dalton Trans.* **49**, 14723–14730 (2020).
- Arnanz, A., Pintado-Sierra, M., Corma, A., Iglesias, M. & Sánchez, F. Bifunctional metal organic framework catalysts for multistep reactions: MOF-Cu(BTC)-[Pd] catalyst for one-pot heteroannulation of acetylenic compounds. *Adv. Synth. Catal.* **354**, 1347–1355 (2012).
- Rasero-Almansa, A. M., Corma, A., Iglesias, M. & Sanchez, F. One-pot multifunctional catalysis with NNN-pincer Zr-MOF: Zr base catalyzed condensation with Rh-catalyzed hydrogenation. *ChemCatChem* **5**, 3092–3100 (2013).
- Qin, Y., Hao, M., Xu, C. & Li, Z. Visible light initiated oxidative coupling of alcohols and *o*-phenylenediamines to synthesize benzimidazoles over MIL-101(Fe) promoted by plasmonic Au. *Green Chem.* **23**, 4161–4169 (2021).

29. Wang, D., Albero, J., García, H. & Li, Z. Visible-light-induced tandem reaction of *o*-aminothiophenols and alcohols to benzothiazoles over Fe-based MOFs: Influence of the structure elucidated by transient absorption spectroscopy. *J. Catal.* **349**, 156–162 (2017).
30. Chen, R., Jalili, Z. & Tayebee, R. UV-visible light-induced photochemical synthesis of benzimidazoles by coomassie brilliant blue coated on W-ZnO@NH₂ nanoparticles. *RSC Adv.* **11**, 16359–16375 (2021).
31. Qin, Y., Hao, M., Ding, Z. & Li, Z. Pt@MIL-101(Fe) for efficient visible light-initiated coproduction of benzimidazoles and hydrogen from the reaction between *o*-phenylenediamines and alcohols. *J. Catal.* **410**, 156–163 (2022).
32. Toyao, T., Saito, M., Horiuchi, Y. & Matsuoka, M. Development of a novel one-pot reaction system utilizing a bifunctional Zr-based metal-organic framework. *Catal. Sci. Technol.* **4**, 625–628 (2014).
33. Wang, D. & Li, Z. Bi-functional NH₂-MIL-101(Fe) for one-pot tandem photo-oxidation/Knoevenagel condensation between aromatic alcohols and active methylene compounds. *Catal. Sci. Technol.* **5**, 1623–1628 (2015).
34. Daliran, S., Khajeh, M., Oveisi, A. R., García, H. & Luque, R. Porphyrin catecholate iron-based metal-organic framework for efficient visible light-promoted one-pot tandem C–C couplings. *ACS Sustain. Chem. Eng.* **10**, 5315–5322 (2022).
35. Chahkamali, F. O., Sobhani, S. & Sansano, J. M. A novel base-metal multifunctional catalyst for the synthesis of 2-amino-3-cyano-4*H*-chromenes by a multicomponent tandem oxidation process. *Sci. Rep.* **12**, 1–20 (2022).
36. Moghadam, H. H., Sobhani, S. & Sansano, J. M. New nanomagnetic heterogeneous cobalt catalyst for the synthesis of aryl nitriles and biaryls. *ACS Omega* **5**, 18619–18627 (2020).
37. Sobhani, S., Zarei, H. & Sansano, J. M. A new nanomagnetic Pd-Co bimetallic alloy as catalyst in the Mizoroki-Heck and Buchwald-Hartwig amination reactions in aqueous media. *Sci. Rep.* **11**, 1–21 (2021).
38. Rouzifar, M., Sobhani, S., Farrokhi, A. & Sansano, J. M. Fe-MIL-101 modified by isatin-Schiff-base-Co: A heterogeneous catalyst for C–C, C–O, C–N, and C–P cross coupling reactions. *New J. Chem.* **45**, 19963–19976 (2021).
39. Zhang, Z., Li, X., Liu, B., Zhao, Q. & Chen, G. Hexagonal microspindle of NH₂-MIL-101(Fe) metal-organic frameworks with visible-light-induced photocatalytic activity for the degradation of toluene. *RSC Adv.* **6**, 4289–4295 (2016).
40. Wang, J. *et al.* Co (II) complexes loaded into metal-organic frameworks as efficient heterogeneous catalysts for aerobic epoxidation of olefins. *Catal. Sci. Technol.* **6**, 161–168 (2016).
41. Han, Y., Zhai, J., Zhang, L. & Dong, S. Direct carbonization of cobalt-doped NH₂-MI-53(Fe) for electrocatalysis of oxygen evolution reaction. *Nanoscale* **8**, 1033–1039 (2016).
42. Kowalski, G., Pielichowski, J. & Grzesik, M. Characteristics of polyaniline cobalt supported catalysts for epoxidation reactions. *Sci. World J.* 1–9 (2014).
43. Cai, X., Wang, H., Zhang, Q., Tong, J. & Lei, Z. Magnetically recyclable core-shell Fe₃O₄@chitosan-Schiff base complexes as efficient catalysts for aerobic oxidation of cyclohexene under mild conditions. *J. Mol. Catal. A: Chem.* **383**, 217–224 (2014).
44. Dong, S. *et al.* Visible-light-induced catalytic transfer hydrogenation of aromatic aldehydes by palladium immobilized on amine-functionalized iron-based metal-organic frameworks. *ACS Appl. Nano Mater.* **1**, 4247–4257 (2018).
45. Qi, Z., Yang, Y., Miao, T., Li, L. & Fu, X. Progress in photocatalytic synthesis of benzimidazoles. *ChemistrySelect* **6**, 12628–12643 (2021).
46. Skolia, E., Apostolopoulou, M. K., Nikitas, N. F. & Kokotos, C. G. Photochemical synthesis of benzimidazoles from diamines and aldehydes. *Eur. J. Org. Chem.* **3**, 422–428 (2021).
47. Mortimer, C. G. *et al.* Antitumor benzothiazoles. 2-(3,4-dimethoxyphenyl)-5 fluorobenzothiazole (GW 610, NSC 721648), a simple fluorinated 2-arylbenzothiazole, shows potent and selective inhibitory activity against lung, colon, and breast cancer cell lines. *J. Med. Chem.* **49**, 179–185 (2006).
48. Wright, J. B. The chemistry of the benzimidazoles. *Chem. Rev.* **48**, 397–541 (1951).
49. Tzani, M. A., Gabriel, C. & Lykakis, I. N. Selective synthesis of benzimidazoles from *o*-phenylenediamine and aldehydes promoted by supported gold nanoparticles. *Nanomaterials* **10**, 2405–2421 (2020).
50. Alaqeel, S. I. Synthetic approaches to benzimidazoles from *o*-phenylenediamine. *J. Saudi Chem. Soc.* **21**, 229–237 (2017).
51. Liu, M. *et al.* Crystalline covalent triazine frameworks by in situ oxidation of alcohols to aldehyde monomers. *Angew. Chem. Int. Ed.* **57**, 11968–11972 (2018).
52. Maiti, B. & Chanda, K. Diversity oriented synthesis of benzimidazole-based biheterocyclic molecules by combinatorial approach. *RSC Adv.* **6**, 50384–50413 (2016).
53. Dehbanipour, Z. & Zarnegareyan, A. Magnetic nanoparticles supported a palladium bis (benzothiazole) complex: A novel efficient and recyclable catalyst for the synthesis of benzimidazoles and benzothiazoles from benzyl alcohol. *Inorg. Chem. Commun.* **141**, 109513–109523 (2022).
54. Mobinikhaledi, A., Moghanian, H., Ghazvini, S. M. B. H. & Dalvand, A. Copper containing poly (melamine-terephthaldehyde)-magnetite mesoporous nanoparticles: A highly active and recyclable catalyst for the synthesis of benzimidazole derivatives. *J. Porous Mater.* **25**, 1123–1134 (2018).
55. Madgula, K., Dandula, S., Kasula, S. & Halady, P. Microwave synthesized ionic liquids as green catalysts for the synthesis of benzimidazoles: Spectral and computational studies for potential anticancer activity. *Inorg. Chem. Commun.* **138**, 109218–109224 (2022).
56. Dhopte, K. B., Zambare, R. S., Patwardhan, A. V. & Nemade, P. R. Role of graphene oxide as a heterogeneous acid catalyst and benign oxidant for synthesis of benzimidazoles and benzothiazoles. *RSC Adv.* **6**, 8164–8172 (2016).
57. Vallés-García, C. *et al.* Nitro functionalized chromium terephthalate metal-organic framework as multifunctional solid acid for the synthesis of benzimidazoles. *J. Colloid. Interface Sci.* **560**, 885–893 (2020).
58. Preston, P. N. Synthesis, reactions, and spectroscopic properties of benzimidazoles. *Chem. Rev.* **74**, 279–314 (1974).
59. Parghi, K. D. & Jayaram, R. V. Sequential oxidation and condensation of alcohols to benzimidazoles/benzodiazepines by MoO₃-SiO₂ as a heterogeneous bifunctional catalyst. *Catal. Commun.* **11**, 1205–1210 (2010).
60. Das, S., Mallick, S. & De Sarkar, S. Cobalt-catalyzed sustainable synthesis of benzimidazoles by redox-economical coupling of *o*-nitroanilines and alcohols. *J. Org. Chem.* **84**, 12111–12119 (2019).
61. Benzekri, Z. *et al.* NH₃(CH₂)₅NH₃BiCl₅: An efficient and recyclable catalyst for the synthesis of benzoxazole, benzimidazole and benzothiazole heterocycles. *J. Iran. Chem. Soc.* **15**, 2781–2787 (2018).
62. Jiang, J., Liang, Z., Xiong, X., Zhou, X. & Ji, H. A carbazolyl porphyrin-based conjugated microporous polymer for metal-free photocatalytic aerobic oxidation reactions. *ChemCatChem* **12**, 3523–3529 (2020).
63. Khoshnavazi, R., Bahrami, L. & Havasi, F. Organic-inorganic hybrid polyoxometalate and its graphene oxide-Fe₃O₄ nanocomposite, synthesis, characterization and their applications as nanocatalysts for the Knoevenagel condensation and the synthesis of 2, 3-dihydroquinazolin-4 (1*H*)-ones. *RSC Adv.* **6**, 100962–100975 (2016).
64. Muralidhar, L. & Girija, C. R. Simple and practical procedure for Knoevenagel condensation under solvent-free conditions. *J. Saudi Chem. Soc.* **18**, 541–544 (2014).
65. Furst, A. L. & Rancis, M. B. Impedance-based detection of bacteria. *Chem. Rev.* **119**, 700–726 (2019).
66. Franci, G. *et al.* Silver nanoparticles as potential antibacterial agents. *Molecules* **20**, 8856–8874 (2015).
67. Zhang, J. M. *et al.* Antibacterial ability and cytocompatibility of Cu-incorporated Ni-Ti-O nanopores on Ni Ti alloy. *Rare Met.* **38**, 552–560 (2019).
68. Gupta, A., Mumtaz, S., Li, C. H., Hussain, I. & Rotello, V. M. Combatting antibiotic-resistant bacteria using nanomaterials. *Chem. Soc. Rev.* **48**, 415–427 (2019).

69. Han, H. *et al.* Shining light on transition metal sulfides: New choices as highly efficient antibacterial agents. *Nano Res.* **14**, 2512–2534 (2021).
70. Elgohary, E. A. *et al.* A review of the use of semiconductors as catalysts in the photocatalytic inactivation of microorganisms. *Catalysts* **11**, 1498–1512 (2021).
71. Liu, J. *et al.* Visible-light driven rapid bacterial inactivation on red phosphorus/titanium oxide nanofiber heterostructures. *J. Hazard. Mater.* **413**, 125462–125471 (2021).
72. Yan, L. *et al.* Metal organic frameworks for antibacterial applications. *Chem. Eng. J.* **435**, 134975–134989 (2022).
73. Li, P. *et al.* Metal-organic frameworks with photocatalytic bactericidal activity for integrated air cleaning. *Nat. Commun.* **10**, 1–10 (2019).

Acknowledgements

We thank University of Birjand Research Council for supporting of this work, Spanish Ministerio de Economía, Industria Competitividad, Agencia Estatal de Investigación (AEI) and Fondo Europeo de Desarrollo Regional (FEDER, EU) (PID2019-107268GB-I00), University of Alicante for the access to the FESEM, EDX, mapping, TEM and XPS facilities, and also Prof. Hermenegildo García from Universitat Politècnica de Valencia for the EPR analysis.

Author contributions

S.S. is the research supervisor and the corresponding author. All the synthesis was done by M.R. A.F. contributed to the general discussion. J.M.S. performed the XPS, TEM, EDX, mapping, and FESEM analysis. All the authors reviewed the manuscript.

Competing interests

The authors declare no competing interests.

Additional information

Supplementary Information The online version contains supplementary material available at <https://doi.org/10.1038/s41598-023-32241-z>.

Correspondence and requests for materials should be addressed to S.S.

Reprints and permissions information is available at www.nature.com/reprints.

Publisher's note Springer Nature remains neutral with regard to jurisdictional claims in published maps and institutional affiliations.



Open Access This article is licensed under a Creative Commons Attribution 4.0 International License, which permits use, sharing, adaptation, distribution and reproduction in any medium or format, as long as you give appropriate credit to the original author(s) and the source, provide a link to the Creative Commons licence, and indicate if changes were made. The images or other third party material in this article are included in the article's Creative Commons licence, unless indicated otherwise in a credit line to the material. If material is not included in the article's Creative Commons licence and your intended use is not permitted by statutory regulation or exceeds the permitted use, you will need to obtain permission directly from the copyright holder. To view a copy of this licence, visit <http://creativecommons.org/licenses/by/4.0/>.

© The Author(s) 2023